

# Quantitative Proton Radiography and Shadowgraphy for Arbitrary Intensities

J. R. Davies,<sup>1</sup> P. V. Heuer,<sup>1</sup> and A. F. A. Bott<sup>2</sup>

<sup>1</sup>Laboratory for Laser Energetics, University of Rochester

<sup>2</sup>Clarendon Laboratory, University of Oxford

Charged-particle radiography, most commonly with protons, and shadowgraphy are widely used in laser-plasma experiments to infer electric and magnetic fields and electron density, respectively. For many experiments of interest, intensity modulations due to absorption and scattering of the charged particles or photons can be neglected; therefore, intensity modulations are caused by deflections in the plasma. Deflection at the detector can then be expressed in terms of a path-integrated transverse Lorentz force for charged-particle radiography and a path-integrated transverse refractive index gradient for shadowgraphy. We will adopt the generic term deflectometry to describe both charged-particle radiography and shadowgraphy in the regime where intensity modulations are due principally to deflection.

A number of papers in plasma physics have used direct inversion of deflectometry data to obtain a path-integrated Lorentz force or refractive index gradient. These direct inversion algorithms find a minimum deflection solution where trajectories do not cross. Therefore, if trajectories did cross, the direct inversion may not reproduce the actual profiles. Direct inversion, however, does provide one possible solution to what is then a degenerate problem, subject to known constraints, which can be useful information. Most of these direct-inversion codes are publicly available.<sup>1–5</sup> These papers concentrate on proton radiography, with only one explicitly considering shadowgraphy,<sup>1</sup> and none considering the possibility of radiography with a relativistic particle, which is possible in laser-plasma experiments using electrons from a laser-plasma accelerator.

From a mathematical point of view, the direct-inversion problem was first formulated in a paper by Monge published in 1781,<sup>6</sup> and then in a modern mathematical manner by Kantorovich in 1942,<sup>7</sup> leading to the name Monge–Kantorovich problem or, more descriptively, the optimal transport problem. Monge and Kantorovich both considered finding the minimum cost for leveling a land area as an application of the theory. Kantorovich added “location of consumption stations with respect to production stations” as a second application of the theory. Since then, numerous applications have been found, of which direct inversion of deflectometry data by minimizing total deflection is perhaps the most recent.

The majority of the publicly available direct-inversion codes<sup>3–5</sup> solve the Monge–Ampère equation first derived by Monge and then stated in a more-general form by Ampère in 1819, although the numerical algorithm used in these codes was only published in 2011.<sup>8</sup> The Poisson equations considered by some authors,<sup>1,2</sup> and frequently mentioned in texts discussing shadowgraphy, can be considered special cases of the Monge–Ampère equation, valid in the limit of very small deflections.

If we consider the problem in terms of the data, then direct inversion comes down to determining the movement of counts in detector bins that map the source intensity  $I_0$  (the signal on the detector in the absence of an object) to the measured intensity  $I$ , or vice versa. From this point of view, and from the perspective of a plasma physicist, it occurred to us that an algorithm based on an electrostatic plasma model should always be able to obtain a solution. The source or measured intensity can be treated as an initial electron distribution and the other intensity as a fixed ion distribution. Electrostatic forces will then cause the electron distribution to evolve to the ion distribution. The displacement of the electrons from their initial to their equilibrium positions will give the deflections at the detector. Oscillations about the desired equilibrium positions can be damped by applying drag to

the electrons. Electrostatic plus kinetic energy will decay steadily and go to zero in equilibrium since drag removes energy from the system, providing a simple convergence criterion.

The first scheme that occurred to us was an electrostatic particle-in-cell (PIC) code with the addition of electron drag; because this is a common type of code in plasma physics, efficient, robust algorithms exist, and it could make use of existing codes. We then considered a fluid code as a potentially faster, less memory-intensive alternative. A Lagrangian scheme, where the numerical grid moves with the fluid, provides the most direct method of determining the deflections. A Eulerian scheme, where the numerical grid is fixed, would require tracking the center of mass of the initial fluid elements in every cell, and so could require more calculations than a PIC code. Therefore, we also implemented a Lagrangian fluid scheme. We started with 1-D codes as a quick method to test the algorithms before writing 2-D codes.

To make a fair comparison of the electrostatic algorithm to the Sulman, Williams, and Russell algorithm for solving the Monge–Ampère equation,<sup>3–5,8</sup> we returned to the original *MATLAB* script of *PROBLEM*, which is not provided on GitHub, and added an inbuilt convergence criterion and an adaptive time step. We also compared our codes to the power-diagram algorithm,<sup>1</sup> which uses weighted Voronoi, or power diagrams of the intensities to determine the deflections at the detector.

Our codes output what we refer to as a dimensionless line-integrated transverse force. For charged-particle radiography,

$$\mathcal{F}_x = \frac{L}{Mw_x} \frac{q}{p\bar{v}} \int E_x - vB_y dz, \quad \mathcal{F}_y = \frac{L}{Mw_y} \frac{q}{p\bar{v}} \int E_y - vB_x dz,$$

which is valid for a relativistic particle. For shadowgraphy,

$$\mathcal{F}_x = \frac{L}{Mw_x} \frac{1}{2} \int \frac{\partial n'_e / \partial x}{1 - n'_e} dz, \quad \mathcal{F}_y = \frac{L}{Mw_y} \frac{1}{2} \int \frac{\partial n'_e / \partial y}{1 - n'_e} dz,$$

where  $L$  is the object-to-detector distance,  $M$  is magnification,  $w$  is the detector pixel width in the object plane,  $q$  is the charge,  $p$  is momentum,  $v$  is velocity,  $z$  is the probing axis, and  $n'_e = n_e/n_c$ , where  $n_e$  is electron density and  $n_c$  is critical density for the shadowgraphy probe.

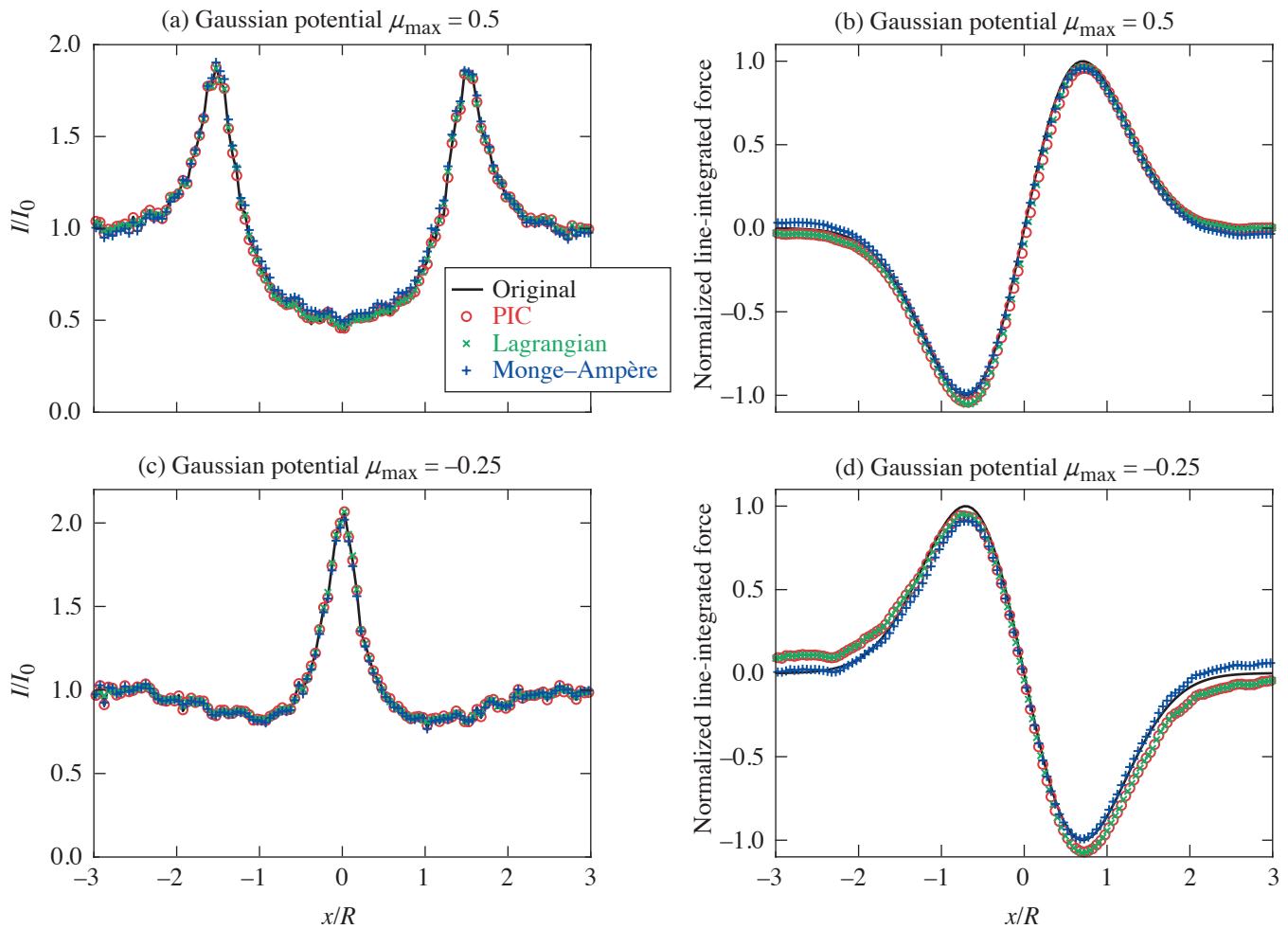
Our codes are written in *MATLAB* and are publicly available.<sup>9</sup> Python versions of the 2-D PIC code and the Monge–Ampère code are under development.<sup>10</sup>

To test the codes, we used synthetic radiographs that we had generated previously by proton tracing in specified radial forces in cylindrical and spherical geometry for a range of profiles and amplitudes,<sup>11</sup> which are publicly available as hdf5 files in prad-format.<sup>12</sup> The force is expressed as a dimensionless parameter  $\mu$

$$\mu = \frac{2LF}{Mp\bar{v}}, \quad \mu = -\frac{L}{M} \frac{dn'_e/dr}{1 - n'_e}$$

for charged-particle radiography and shadowgraphy, respectively. Results for cylindrical Gaussian potentials with  $\mu_{\max} = 0.5$  (defocusing) and  $-0.25$  (focusing), values where trajectories do not cross, are shown in Fig. 1. All of our codes accurately reproduced the measured intensity and the line-integrated transverse force to within the noise level of the original intensity. We carried out an extensive range of tests intended to push the limits of the codes.

Only the PIC code obtained a solution for every case. The 2-D Lagrangian code failed for large-intensity modulations, but was faster than the 2-D PIC code without massively parallel processing, which would be possible with a PIC code. The Monge–Ampère code was considerably faster than the electrostatic codes in 2-D without massively parallel processing, but failed for intensities with extensive regions of zero signal, high contrast ratios, or large deflections across the boundaries, and could not obtain the



E30464JR

Figure 1

Results for a cylindrical Gaussian potential [(a),(c)] intensity profiles and [(b),(d)] line-integrated transverse force normalized so that the maximum of the original is 1 for  $\mu_{\max} = 0.5$  and  $-0.25$ , respectively.

same degree of convergence to the measured intensity as the electrostatic codes. The power-diagram code was by far the slowest and failed for large peaks in the intensity. In 1-D, however, the Lagrangian code was the fastest and always obtained a solution.

Our final recommendations are to use the Monge–Ampère code to take a quick first look at data, and to use the PIC code if the Monge–Ampère code fails or a more-accurate inversion is desired. In the rare case of 1-D problems, the Lagrangian code is the best option.

This material is based upon work supported by the Department of Energy, under Award Number DE-SC0020431, by the Department of Energy National Nuclear Security Administration under Award Number DE-NA0003856, the University of Rochester, and the New York State Energy Research and Development Authority.

1. M. F. Kasim *et al.*, Phys. Rev. E **95**, 023306 (2017).
2. C. Graziani *et al.*, Rev. Sci. Instrum. **88**, 123507 (2017); PRaLine Code (Proton Radiography Linear Reconstruction, the “reconstruction” is silent), Accessed 03 March 2023, <https://github.com/flash-center/PRaLine>.

3. M. F. Kasim, Invert Shadowgraphy and Proton Radiography, Accessed 03 March 2023, <https://github.com/mfkasim1/invert-shadowgraphy>.
4. A. F. A. Bott *et al.*, *J. Plasma Phys.* **83**, 905830614 (2017); PROBLEM Solver (PROton-imaged B-field nonLinear Extraction Module), Accessed 03 March 2023, <https://github.com/flash-center/PROBLEM>.
5. M. F. Kasim *et al.*, *Phys. Rev. E* **100**, 033208 (2019); M. F. Kasim, PRNS (Proton Radiography with No Source), Accessed 03 March 2023, <https://github.com/OxfordHED/proton-radiography-no-source>.
6. G. Monge, *Mém. de l'Ac. R. des. Sc. An.* **1**, 666 (1781).
7. L. Kantorovitch, *Manage. Sci.* **5**, 1 (1958).
8. M. M. Sulman, J. F. Williams, and R. D. Russell, *Appl. Numer. Math.* **61**, 298 (2011).
9. J. R. Davies, A 1-D Electrostatic PIC Code for Direct Inversion of Deflectometry Data (Version 2), Zenodo, Accessed 7 March 2023, <http://doi.org/10.5281/zenodo.6638904>; J. R. Davies, A 2-D Electrostatic PIC Code for Direct Inversion of Deflectometry Data (Version 1), Zenodo, Accessed 7 March 2023, <http://doi.org/10.5281/zenodo.6638812>; J. R. Davies, A 1-D Electrostatic, Lagrangian Two-Fluid Code for the Direct Inversion of Deflectometry Data (Version 1), Zenodo, Accessed 7 March 2023, <http://doi.org/10.5281/zenodo.6638911>; J. R. Davies, A 2-D Electrostatic Lagrangian Two-Fluid Code for the Direct Inversion of Deflectometry Data (Version 1), Zenodo, Accessed 7 March 2023, <https://doi.org/10.5281/zenodo.6638929>; J. R. Davies and A. F. A. Bott, A Matlab Function to Solve the Monge–Ampere Equation Using the Sulman, Williams and Russell Algorithm (Version 1), Zenodo, Accessed 7 March 2023, (<https://doi.org/10.5281/zenodo.6685314>).
10. P. Heuer, InvertDeflectPy: A Collection of Algorithms for Inverting Deflectometry Data, Accessed 7 March 2023, <https://github.com/pheuer/InvertDeflectPy>.
11. J. Davies and P. Heuer, Synthetic Proton Radiographs for Testing Direct Inversion Algorithms, Zenodo, Accessed 7 March 2023, <https://doi.org/10.5281/zenodo.6632986>.
12. P. Feister, Pradformat (Particle Radiography File Format Tools)-MATLAB Package, Accessed 7 March 2023, <https://github.com/sfeister/pradformat/blob/f9b95d1d87f26d01e59ab7f145d414e7043fe488/MATLAB/README.md>.